Briefing Space Weather

2022/05/30

1 Sun

1.1 Responsible: José Cecatto

05/23 – No flare (M/X); Fast wind stream (<= 550 km/s); 7 CME c.h.c. toward the Earth;
05/24 – No flare (M/X); Fast wind stream (<= 450 km/s); 3 CME c.h.c. toward the Earth *;
05/25 – M1 flare; No fast wind stream; 19 CME c.h.c. toward the Earth *,*,*;
05/26 – No flare (M/X); No fast wind stream; 4 CME c.h.c. toward the Earth;
05/27 – No flare (M/X); Fast wind stream (<= 500 km/s); 2 CME c.h.c. toward the Earth;
05/28 – No flare (M/X); Fast wind stream (<= 600 km/s); 7 CME c.h.c. toward the Earth *,*;
05/29 – No flare (M/X); Fast wind stream (<= 550 km/s); 6 CME c.h.c. toward the Earth;
05/30 – No flare (M/X); Fast wind stream (<= 600 km/s); 2 CME c.h.c. toward the Earth;
Prev.: Fast wind stream up to May 31; for the next 2 days quite low (01% M, 01% X) probability of M / X flares; also,
occasionally other CME can present component toward the Earth.
c.h.c. – can have a component; * partial halo; ** halo

2 Sun

2.1 Responsible: Douglas Silva

- WSA-ENLIL (CME 2022-05-21T00:12Z)
  - The simulation results indicate that the flank of CME will reach the DSCOVR mission between 2022-05-24T04:00Z and 2022-05-24T18:00Z.
- WSA-ENLIL (CME 2022-05-23T12:36Z)
  - The simulation results indicate that the flank of CME will reach the DSCOVR mission between 2022-05-28T08:30Z and 2022-05-28T22:30Z.
- WSA-ENLIL (CME 2022-05-25T18:38Z)
  - The simulation results indicate that the flank of CME will reach the DSCOVR mission between 2022-05-27T22:00Z and 2022-05-28T12:00Z.

Buracos coronais (SPoCA : Spatial Possibilistic Clustering Algorithm):

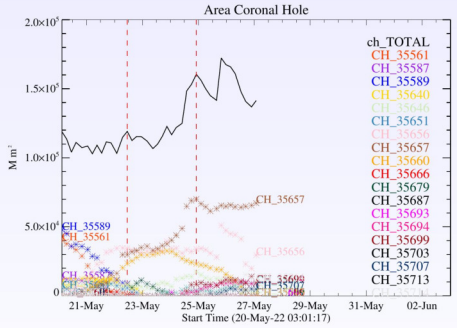

Figura: A linha em preto mostra o resultado da soma das areas para cada intervalo da detecção realizado pelo SPOCA entre os dias 23 e 30 de maio de 2022

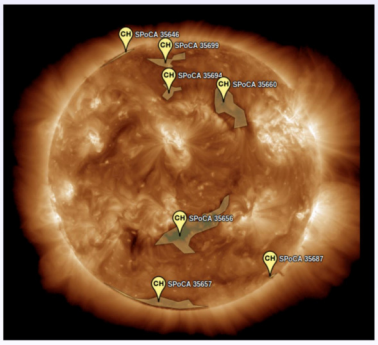

Sobre a imagem em 193 Å do Sol estão destacados os Buracos coronais observados pelo SPOCA por volta das 00:00 UT do dia 25 de maio de 2022.

WSA - ENLIL SPOCA

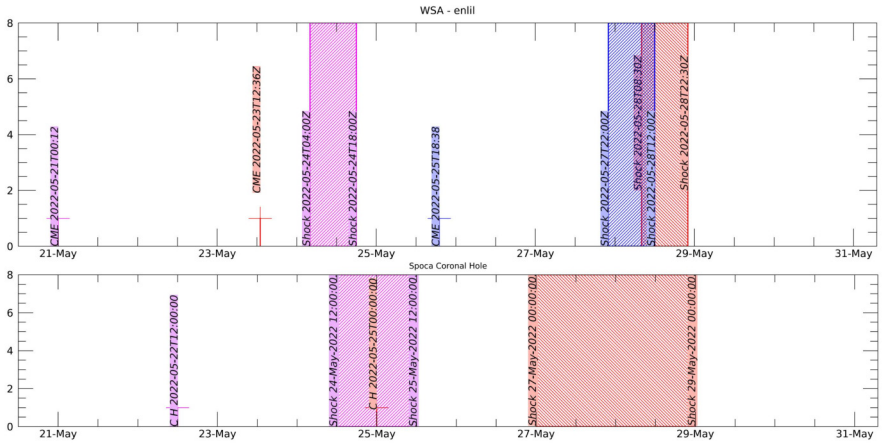

3 Interplanetary Medium

3.1 Responsible: Paulo Jauer

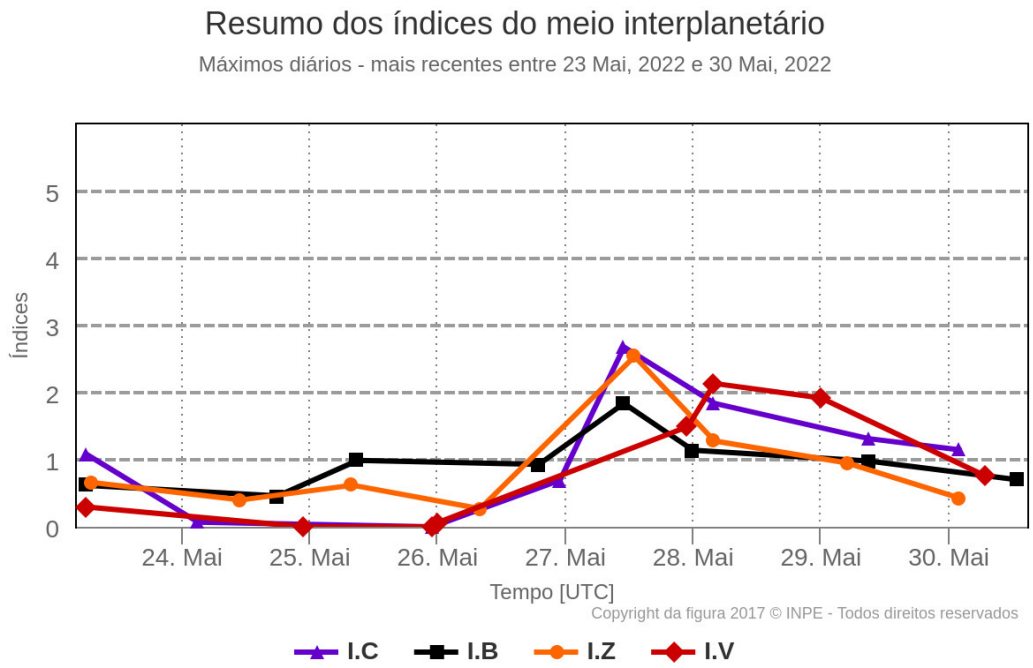

- The interplanetary medium region in the last week showed a low/moderate level of plasma perturbations due to the possible interaction of CME and HSS-like structures identified by the DISCOVR satellite in the interplanetary medium.
- The modulus of the interplanetary magnetic field component showed 1 maximum peak on May 27 at 11:30 from $\sim$ 13.9 nT.
- The Bx/By components showed variations in the analyzed period, both remaining oscillating within the [+10, -10] nT interval, with a change of sector on May 27 at 10:30.
- The component of the bz field showed fluctuations oscillating mostly around zero until close to the 27th/May. After, the bz component, it oscillated in negative average until the beginning of May 30th.
- The solar wind density peaked on May 27 at 09:30 at 42 p/cm^3.
- The solar wind speed fluctuated on average above 400 km/s, with a minimum value on May 27 at 2:30 am of 297 km/s and a maximum value at 1:30 pm on May 30 of 573 km/s.
- The position of the magnetopause was oscillating on average oscillating around the typical 10 Re positions. It showed significant compression on May 27 at 11:36 from 7.63 Re .

4 Radiation Belts

4.1 Responsible: Ligia Alves da Silva

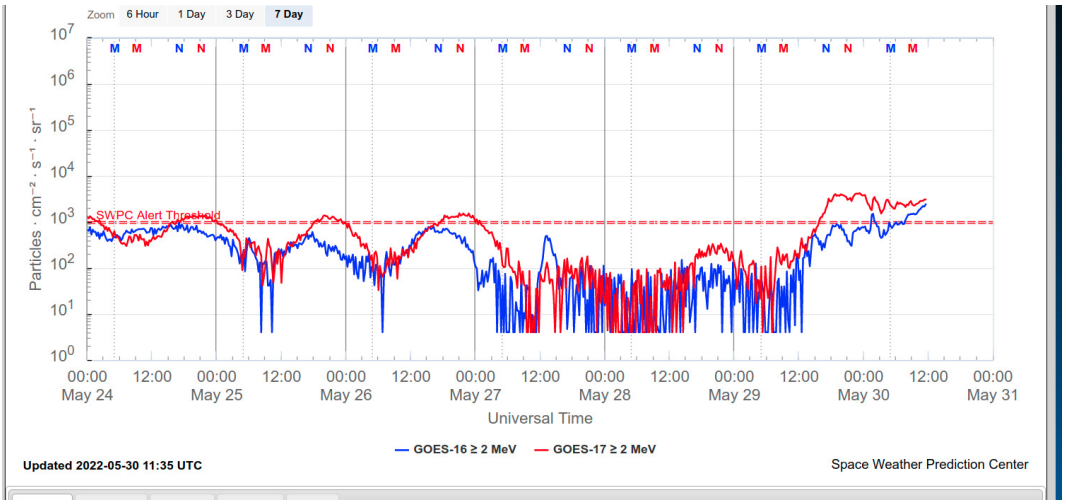

Figura 1: High-energy electron flux (> 2MeV) obtained from GOES-16 and GOES-17 satellite. Source

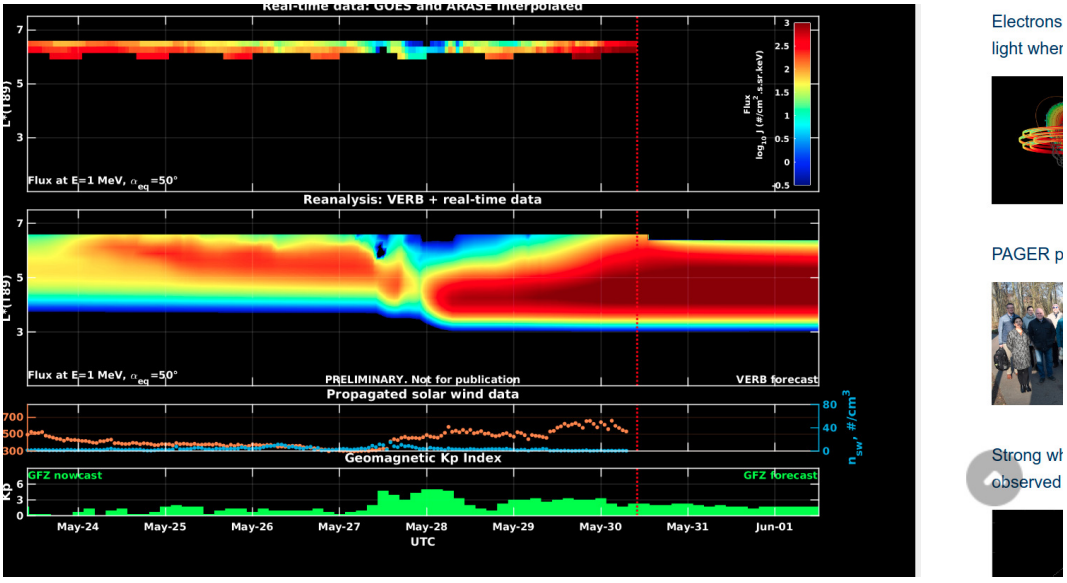

Figura 2: high-energy electron flux data (real-time and interpolated) obtained from ARASE, GOES-16, GOES-17 satellites. Reanalysis's data from VERB code and interpolated electron flux. Solar wind velocity and proton density data from ACE satellite. Source

High-energy electron flux (>2 MeV) in the outer boundary of the outer radiation belt obtained from geostationary satellite data GOES-16 and GOES-17 (Figure 1) is close to 10^3 particles/$(cm^2 ssr)$ on May 24th-26th, presenting two slightly and rapid dropouts on May 25th and 26th, followed by flux recovery. A significant electron flux decrease is observed on May 27th, which is initially influenced by a coronal mass ejection. A rapid increase is observed around 12:00 UT on May 27th, followed by a decrease that persists until May mid-29th. An electron flux increase is observed from 15:00 UT, which exceeds 10^3 particles/$(cm^2 ssr)$ from 12:00 UT.

The GOES-16, GOES-17, and Arase satellite data are analyzed and interpolated to observe the high-energy electron flux variability (1 MeV) in the outer radiation belt (Figure 2). Additionally, the VERB code rebuilds this electron considering the Ultra Low Frequency (ULF) waves' radial diffusion. The simulation (VERB code) shows that the first electron flux decrease observed on May 27th reached

L-shell < 5.5, while the second decrease reached L-shell < 5.5. These electron flux variability occurred concomitantly with the arrival of solar wind structures and ULF wave activities. However, it is important to point out that the data from the ARASE satellite are not available for the week under analysis to confirm the L-shell level of these electron flux variabilities.

5 ULF Waves

5.1 Responsible: José Paulo Marchezi

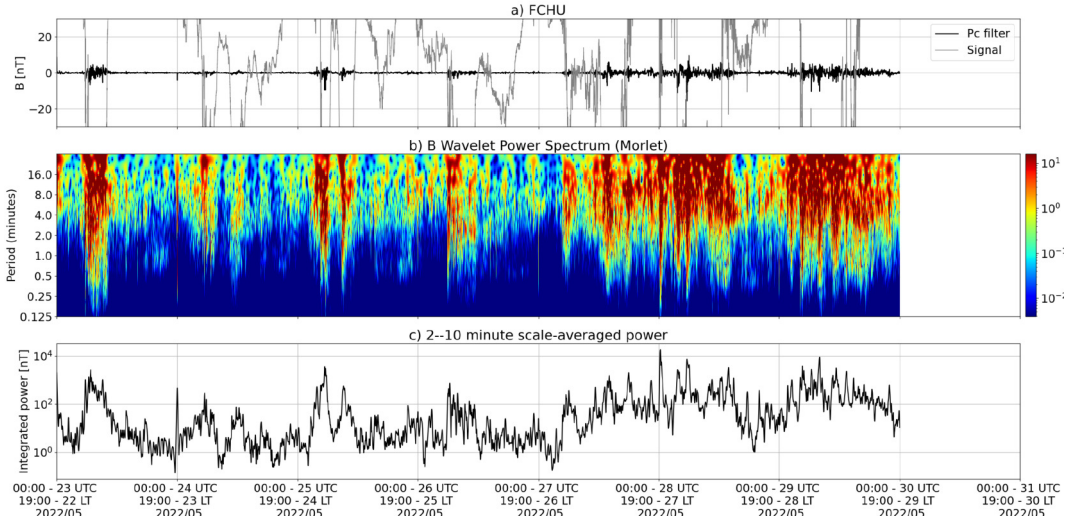

Figura 3: a) signal of the total magnetic field measured in the ISLL Station of the CARISMA network in gray, together with the fluctuation in the range of Pc5 in black. b) Wavelet power spectrum of the filtered signal. c) Average spectral power in the ranges from 2 to 10 minutes (ULF waves).

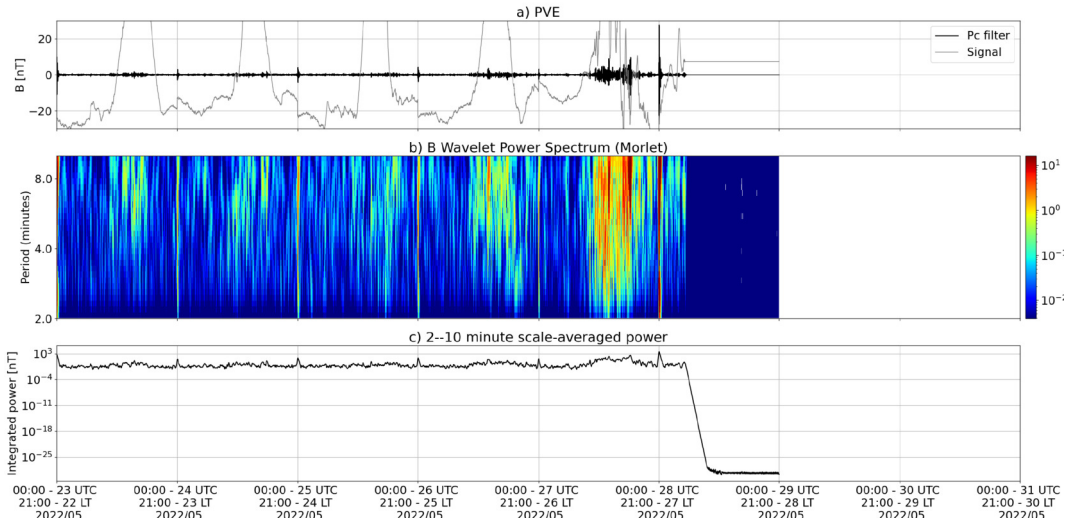

Figura 4: a) signal of the total magnetic field measured in the EMBRACE network in gray, together with the fluctuation in the range of Pc5 in black. b) Wavelet power spectrum of the filtered signal. c) Average spectral power in the ranges from 2 to 10 minutes (ULF waves).

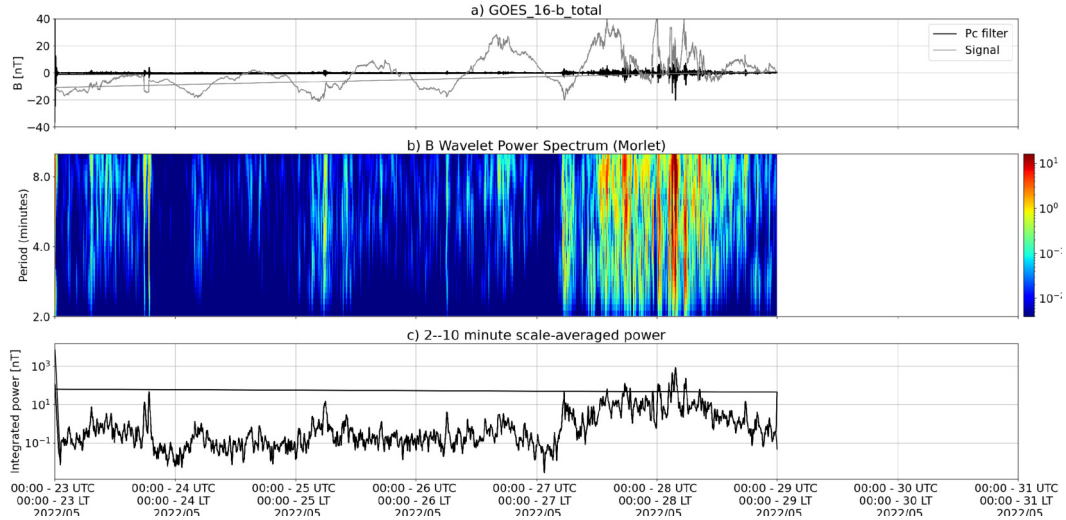

Figura 5: a) signal of the total magnetic field measured by the GOES 16 satellite, together with the fluctuation in the range of Pc5 in black. b) Wavelet power spectrum of the filtered signal. c) Average spectral power in the ranges from 2 to 10 minutes (ULF waves).

During the week, we observed a localized activity of short duration on the 23rd of May - mainly observed at high latitudes. From the 27th of May there is an increase in ULF wave activity, starting with sudden impulses and maintaining activity continuously until the middle of the 28th of May. This activity is observed from high latitudes to low latitudes and by the GOES satellite. Possibly associated with the interaction of a complex structure of the solar wind with the Earth's magnetosphere. Summary 10/10 During the week, we observed a localized activity of short duration on the 23rd of May - mainly observed at high latitudes. From the 27th of May there is an increase in ULF wave activity, starting with sudden impulses and maintaining activity continuously until the middle of the 28th of May. This activity is observed from high latitudes to low latitudes and by the GOES satellite. Possibly associated with the interaction of a complex structure of the solar wind with the Earth's magnetosphere.

6 Ondas EMIC

6.1 Responsible: Claudia Medeiros

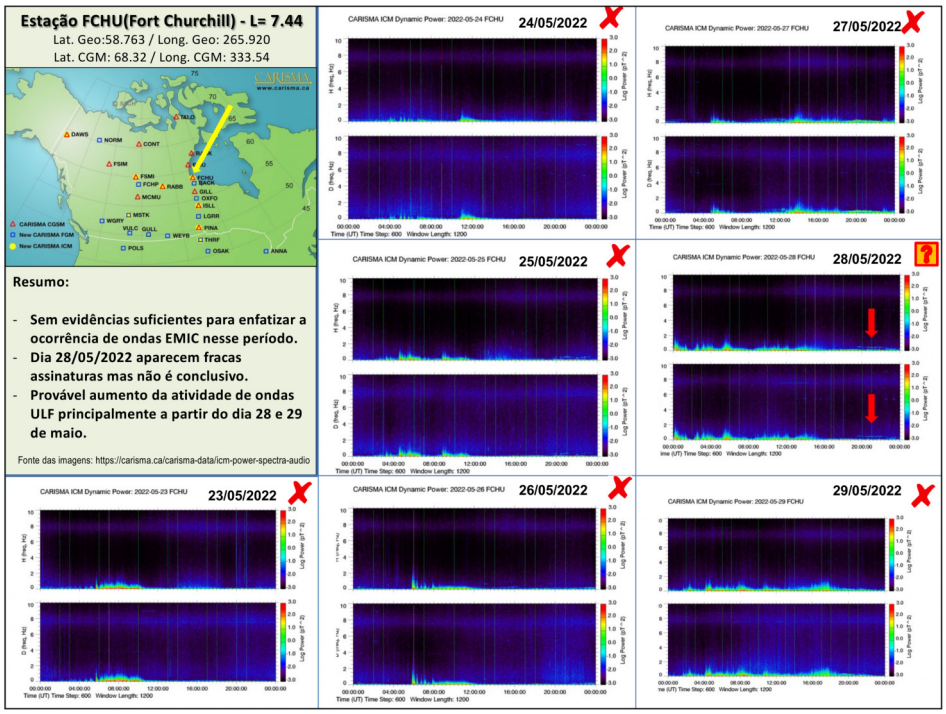

7 Ionosphere

7.1 Responsible: Laysa Resende

Boa Vista:

- There were occurred spread F during all days in this week.
- The Es layers reached scale 3 and 4 during all days in this week.

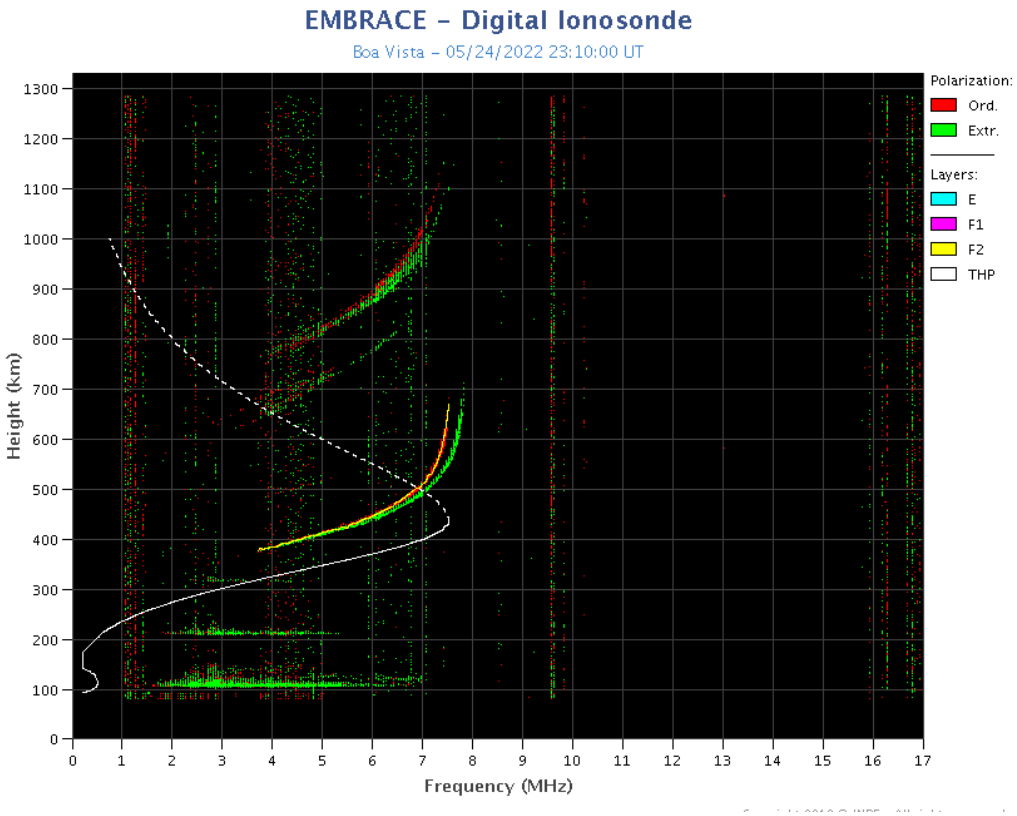

Cachoeira Paulista:

- There were not spread F during this week.
- The Es layers reached scale 2 during this week.

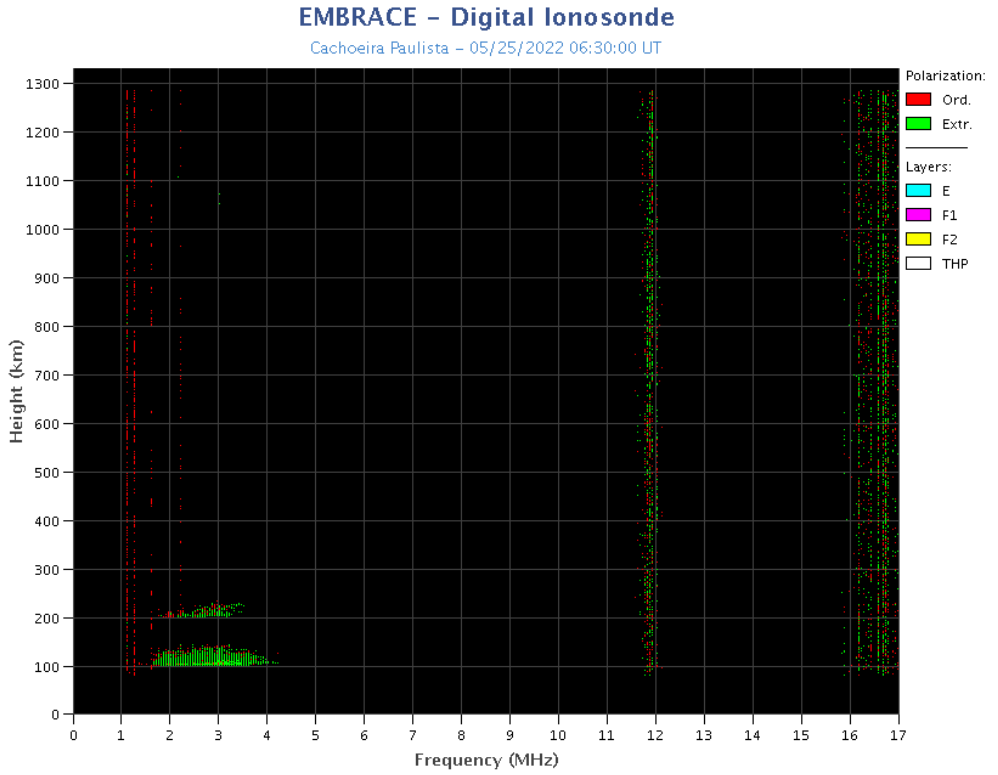

São Luís:

- There were spread F during all days in this week.
- The Es layers reached scale 4 on days 25 and 26.

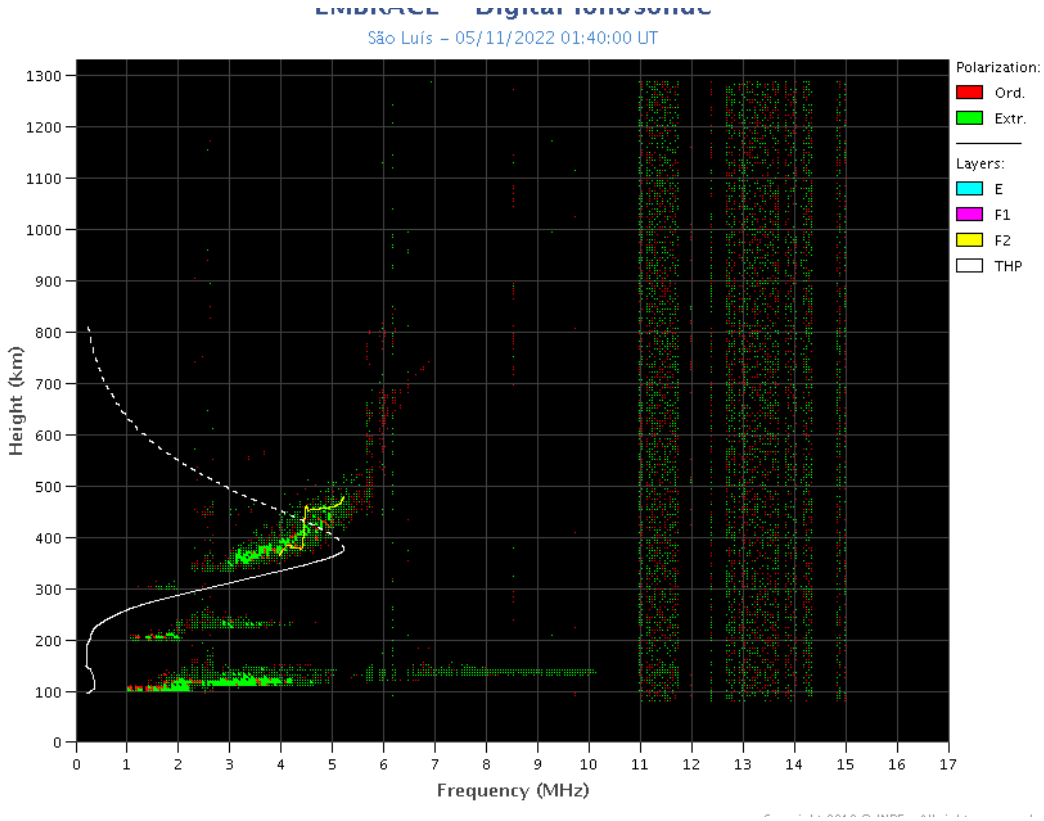

8 Scintilation

8.1 Responsible: Siomel Savio Odriozola

In this report on the S4 scintillation index, data from SLMA in São Luiz/MA, STSN in Sinop/MT, STNT in Natal/RN and SJCE in São José dos Campos/SP are presented. The S4 index tracks the presence of irregularities in the ionosphere having a spatial scale $\sim$ 360 m. The SLMA station showed S4 values below 0.2 throughout the week. On the other hand, STSN had a very similar behavior during the morning of the 25th and 26th (Figure 1). This indicates a non-geophysical cause regarding the S4 values on these two days measured at STSN. Strong and moderate scintillation was recorded in STNT during the last hours of the night on 05/23 and 05/27 respectively. On 05/27, S4 values > 0.5 were recorded during the same time interval in SJCE. Figure 2 shows a sky-map with azimuth, inclination and S4 index values for the GPS constellation satellites that were measured from STNT and SJCE having S4 values above 0.15 and inclinations $> 25°$. It is possible to verify that the greatest contribution to the high values of S4 originates from the northeast direction.

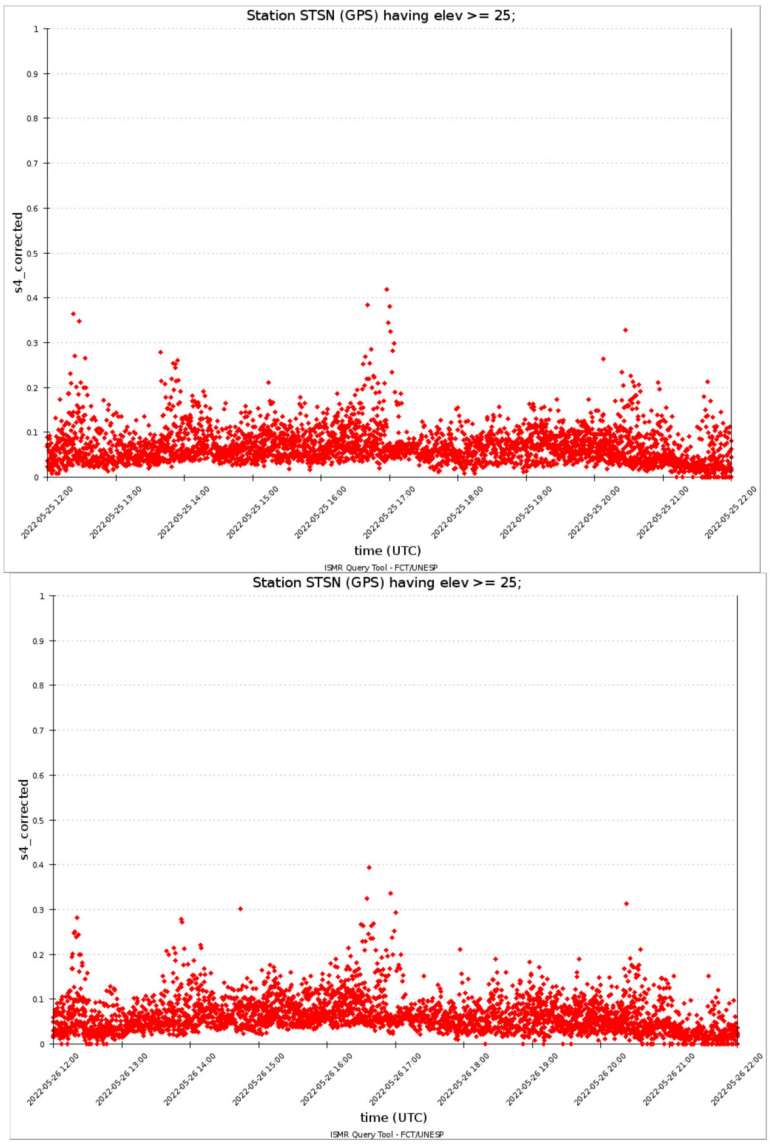

Figura 1: Valores do índice S4 para a constelação GPS para a estação STSN no dia 25/05 (painel superior) e 26/05 (painel superior) entre as 1200-2200 UT.

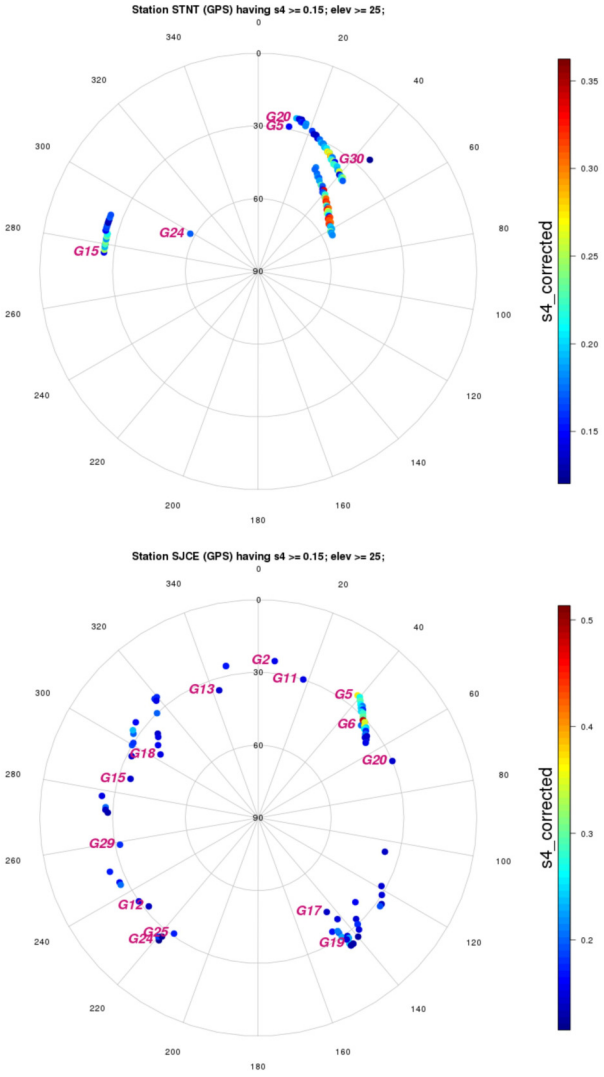

Figura 2: Skymap do índice S4 para a constelação GPS como observados pela estação STNT (painel superior) e a estação SJCE(painel superior) entre as 2200-0300 UT do dia 27/05.

9 All-Sky Imager

9.1 Responsible: LUME

All-Sky Imager EPBs Observation
Observações das EPBs por meio do imageador All-Sky
May 22 - 28, 2022 || 22 - 28 de maio, 2022

Observatory Observatório	May 22 maio 22	May 23 maio 23	May 24 maio 24	May 25 maio 25	May 26 maio 26	May 27 maio 27	May 28 maio 28
CA	✓☁☾	✓☁☾	✓🌥☾	✓☁☾	✓☁☾	✓🌥☾	✓☁✺☾
BJL	✗	✗	✗	✗	✗	✗	✗
CP	✓✺☾	✓✺☾	✓✺☾	✓✺☾	✓☁✺☾	✓☁✺☾	✓✺☾
SMS	✓✺☾	✓✺☾	✓☁☾	✓🌥☾	✓🌧☾	✓🌥☾	✓🌧☾

Definition of Symbols	
CA	São João do Cariri
BJL	Bom Jesus da Lapa
CP	Cachoeira Paulista
SMS	São Martinho da Serra
✓	Observation - Observação
✗	No Observation - Sem Observação
❍	Clear sky - Céu limpo
☁	Partly Cloudy - Parcialmente Nublado

- At the Sao Joao do Cariri observatory no geophysical phenomena such as plasma bubbles and traveling ionospheric disturbances were observed during the period.
- At the Bom de Jesus da Lapa observatory there was no observation due to technical problems.
- At the Cachoeira Paulista observatory no geophysical phenomena such as plasma bubbles and traveling ionospheric disturbances were observed during the period.
- Finally, at the observatory of Sao Martinho da Serra observatory, no geophysical phenomena such as plasma bubbles and traveling ionospheric disturbances were observed during the period.

TEC

- No plasma bubbles were observed during the entire period. As bubble sea- sonality is at the end, thus bubbles have small spatial dimensions and they are difficult to observe on TEC maps. Besides, the equatorial anomaly was observed every day.